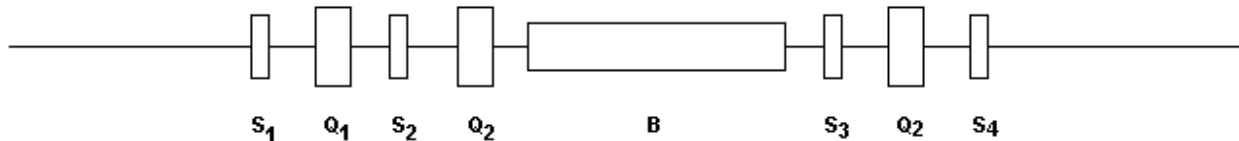


6. Magnets

6.1 Introduction

SESAME will be perhaps erected in steps. The number of steps depends upon the available money. The cheapest way is to use the quadrupole and sextupoles from BESSY I. In this case only new bending magnets with gradients are needed. The next step is to use new quadrupoles and sextupoles in order to increase the length of the long straight sections. It is hoped that the erection of SESAME can start with this step. The structure of the half SESAME-cell and the required specifications of the magnets are given in the following:

The half cell of the storage ring SESAME looks like:



Bending magnet:

Flux density =	1.35 Tesla
Radius =	4.9416 m
Deflection angle =	22.5 degree
Length =	1.9406 m
Strength (k-value) =	0.341 1/m ²

Quadrupole:

Strength (k-value) =	3.00 1/m ²
Gradient =	20 T/m
Magnetic length =	0.23 m

Sextupole:

Strength (m-value) =	52.5 1/m ³
Differ. Gradient =	350 T/m ²
Magnetic length =	0.15 m

For the quadrupoles and sextupoles it is intended to use a design like at ANKA, only the length and the number of coils have to change. A new design has to be performed for the bending magnet and a combined sextupole/quadrupole magnet.

In the following the design of a bending magnet with integrated quadrupole component (defocusing) and a combined sextupole magnet with integrated quadrupole component (defocusing) using a 2D calculation code FEMM for a 2 GeV SESAME storage ring are discussed, the magnets components also investigated at 0.8 GeV injection energy.

6.2 Bending Magnet

The proposed magnet which is shown in Figure (6.1), is a C- shaped magnet with flat parallel ends. The C-shape allows easier extraction of the radiation as well as simple insertion of the dipole vacuum chamber. The magnet yoke is made of laminated steel with low carbon content; the laminations are to minimize the coercive force. The equipotential surface of the pole is calculated

for the desired magnetic field. The scalar potential function $A(x)$ of Equation (6.1) is found for the given dipole (B_o) and quadrupole (g) components and a magnet aperture in the 2-D case.

$$A(x) = B_o y + gxy \quad (6.1)$$

The steel boundaries are shaped according to the equipotential surface (pole profile) as shown in Figure (6.2). The FEMM code is used to calculate the field distribution that meets the specifications of the magnet as shown in Table (6.5a). The nominal value of the dipole field is 1.35T and 2.275T/m as a defocusing quadrupole. A curve fitting for the field distribution in the good field region (within ± 30 mm) is done for the first six harmonics of the field as shown in Figure (6.3). The desired dipole and quadrupole components are then extracted. The width of the poles and the size of the shims are optimised by an iterative technique to reduce the residual field of the higher order harmonics below 1G as shown in Figure (6.4). The field quality for the dipole component ($\Delta B/B$) below 1×10^{-4} and the quadrupole gradient homogeneity in the good field region ($\Delta g/g$) of 1.9×10^{-3} are obtained. The residual field of the higher harmonics at the injection energy of 0.8 GeV is calculated as shown in Figure (6.5) with a field quality of 1×10^{-4} and 1.8×10^{-3} respectively for the dipole and the gradient components.

The coils will be manufactured from a hollow and insulated copper conductor having a cooling channel to minimize a temperature rise of 20°C. Table (6.1) summarises the main electrical and mechanical parameters of the magnet.

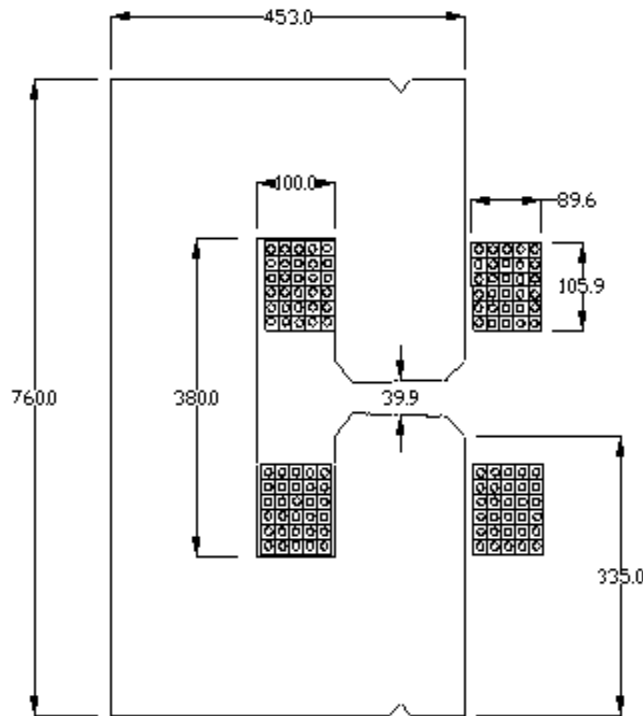
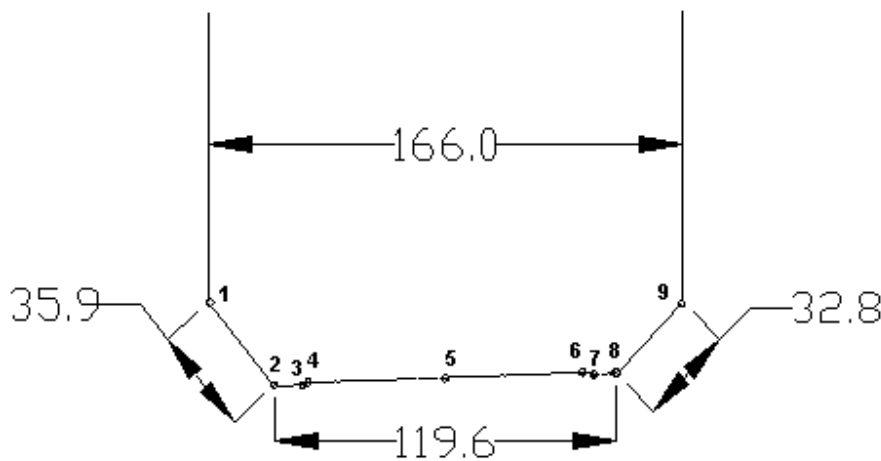


Figure 6.1: The C-shaped dipole magnet

Table 6.1: Bending Magnet Parameters

Parameter	Unit	Value
Magnet Length	m	1.94
Overall Magnet Height	m	0.453
Overall Magnet Width	m	0.76
Pole Face Width	mm	118.8
Magnet Gap	mm	40
Nominal Field	T	1.35
Defocusing Gradient	T/m	2.275
Bending Radius	m	4.942
Bending Angle	Degree	22.50
Number of Coil / Magnet		2
Number of Turn / Coil		30
Current	A	755
Ampere. Turn	A.turn	22635
Current Density	A/mm ²	3.47
Conductor		16 X 16 , Ø 7
Resistance / Coil	mΩ	11.56
Voltage / Coil	V	8.75
Power Consumption / Magnet	kW	13.2
Inductance / Coil	mH	42
Induced voltage / Coil [Ramping Time 3 min]	V	0.1
Water Temp. Rise	°C	20
Pressure Drop / coil	bar	1.75
Water Flow	Litre/min.	2.45
Cooling Circuits		4



	X(mm)	Y(mm)
1	-85.19	43.09
2	-59.8	17.7
3	-50	17.66
4	-48	18.57
5	0	20.21
6	48	21.84
7	52	21.15
8	59.8	21.8
9	83	45

Figure 6.2: Pole face of the bending magnet

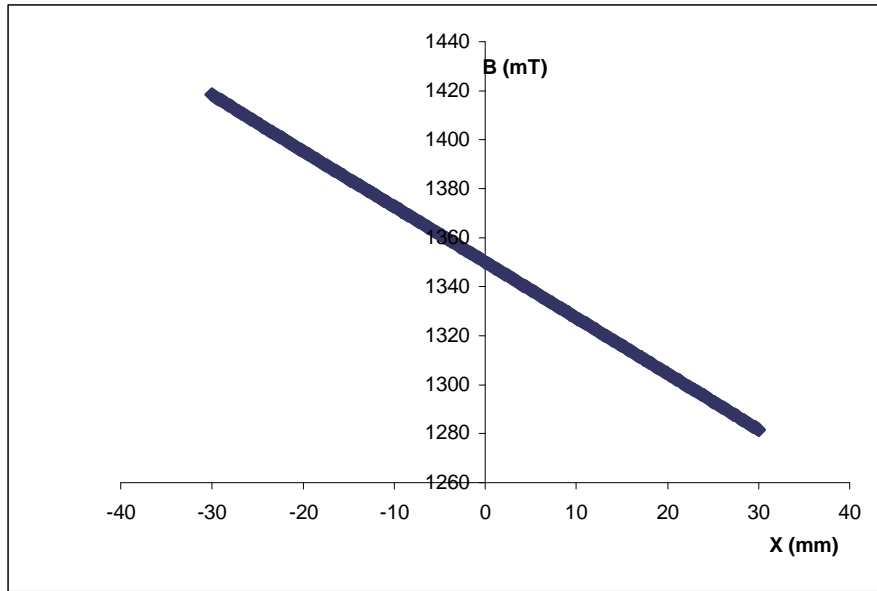


Figure 6.3: The magnetic field distribution at 2 GeV with 1.35 T and - 2.275 T/m

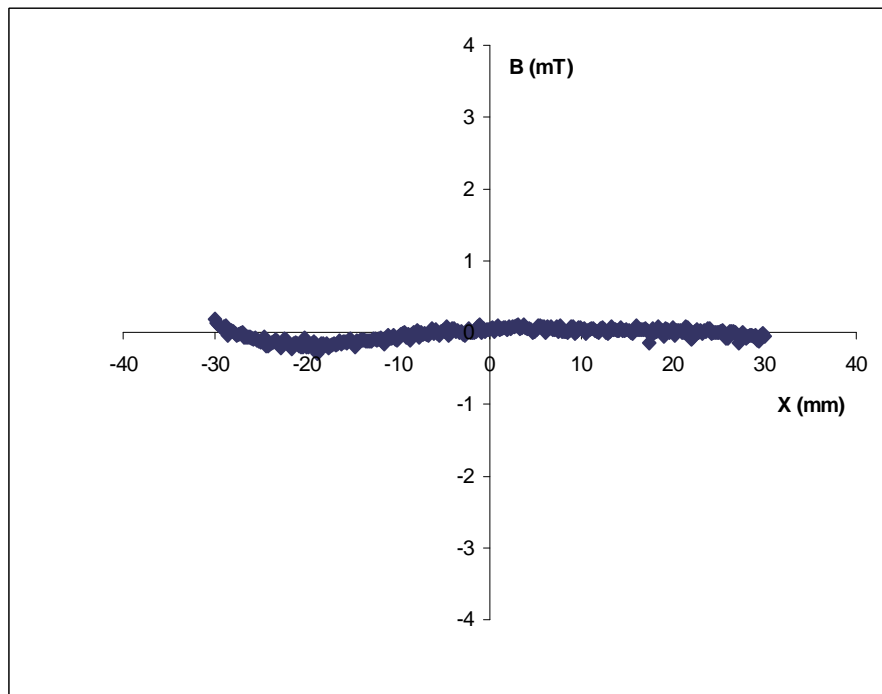


Figure 6.4: The residual field of the higher harmonics at 2 GeV

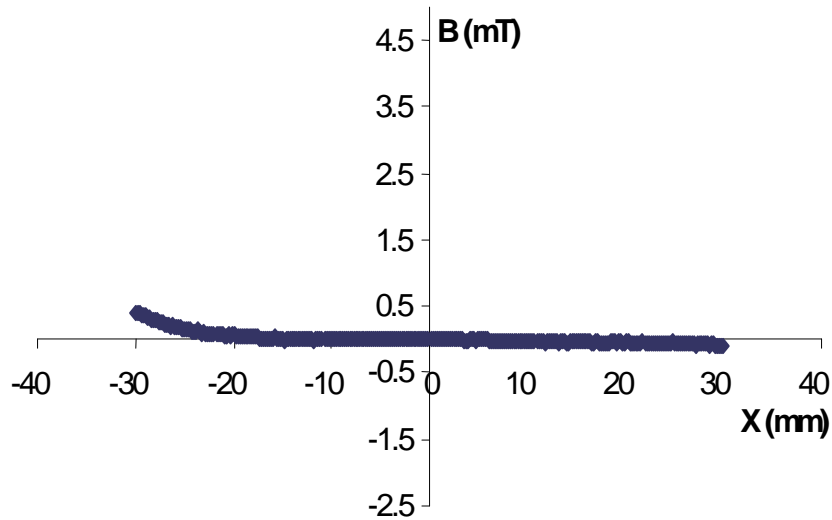


Figure 6.5: The residual field of the higher harmonics at low excitation for 0.8 GeV injection energy with 0.54 T and - 0.91 T/m

6.3 Quadrupole

At present, most of the designed quadrupoles have a gradient of up to 20 T/m. This value leads for a 2GeV machine to maximum quadrupole strength (k) of 3 m^{-2} . Using the ANKA quadrupoles it would mean to reduce the hard edge length to 230 mm or the iron length to 200 mm. The layout of the ANKA quadrupole is presented in Figure (6.6) and the parameters of the SESAME quadrupole is given in Table (6.2).

6.4 Sextupole

The differential gradient of the sextupoles have to be at least 350 T/m^2 . The sextupole of ANKA is presented in Figure (6.7). With 18 windings one gets a differential gradient of 482 T/m^2 . For the requirement of SESAME with 350 T/m^2 , it is possible to reduce the number of windings down to 14. The layout of the ANKA-sextupole is given in Figure (6.7) and the parameters are given in Table (6.3).

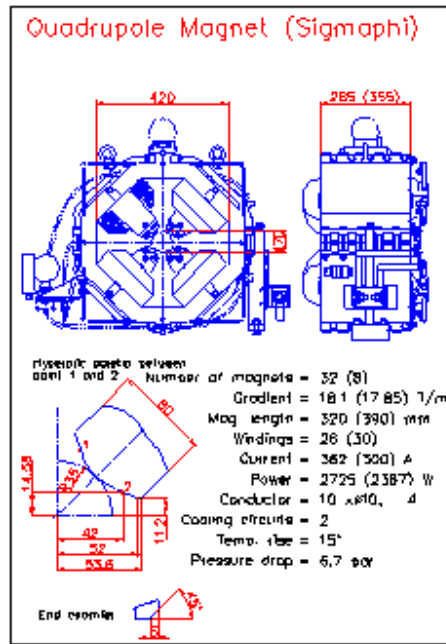


Figure 6.6: Layout of the ANKA-quadrupole

Table 6.2 : Parameters of the SESAME Quadrupole

Parameter	Unit	Type 230
Number of magnets		16
Energy	GeV	2.0
Gradient	T / m	20.0
Magnetic length	m	0.23
Iron length	m	0.20
Total length	m	0.312
Aperture radius	mm	35.0
Pole width	mm	60.0 – 88.0
Iron weight	kg	Ca 300
Ampereturns per pole	A	10 000
Windings per pole		26
Nominal current	A	384.0
Conductor dimensions	mm	10*10, \varnothing =4.0
Conductor / Cooling area	mm ²	87.4 / 12.6
Conductor length	m	76.0
Current density	A/mm ²	4.40
Total resistance	m Ω	15.6
Total inductance	mH	7.7
Time constant	s	0.49
Voltage drop	V	6.00
Power	kW	2.30
Number of cooling circuits		2
Temperature rise	°C	15
Cooling water flow	m ³ /s	22.5*10 ⁻⁶
Cooling water flow	l / h	80.8
Cooling water speed	m / s	1.79
Pressure drop	bar	6.33
Reynold number / critic. veloc. / (m/s)	3580 / 0.625

6.5 Combined Sextupole / Quadrupole Magnet

The combined magnet of Figure (6.6) is used to correct the chromaticity in the vertical plane with a defocusing quadrupole gradient. The scalar potential function $A(x)$ of Equation (6.2) is used to find the equipotential surfaces (pole profile) as shown in Table (6.5b)).

$$A(x) = gxy + g_s (x^2y - y^3/3) \quad (6.2)$$

The nominal values of g and g_s for the quadrupole and sextupole components are 6.17 T/m and 122.4 T/m² respectively. The field distribution in the good field region (within ± 30 mm) is shown in Figure (6.7) for the bending magnet case and a quadrupole gradient homogeneity of 8.9×10^{-4} is obtained as shown in Figure (6.8). The residual field at the injection energy is shown in Figure (6.9) with nominal field values of 2.468 T/m and 48.96 T/m². The magnet is designed with sufficient large yoke width of 64 mm so that the magnetic induction is kept below 1.5 T. Because the quadrupole component is high compared to the sextupole's, the zero field point is shifted from the magnet center of 25 mm, so that the minimum aperture is 34 mm with the pole tip field of 0.354 T. The windings will be manufactured from hollow and insulated copper conductor using a cooling channel to minimize a temperature rise of 20°C. Table (6.4) summarizes the magnet main electrical and mechanical parameters.

Table 6.4: Combined Magnet Parameters

Parameter	Unit	Value
Sextupole type		V
Sext. Gradient	T/m ²	122.4
Quad. Gradient	T/m	6.17
Mag. Length	m	0.2
Overall Mag. Width	m	0.46
Overall Mag. Height	m	0.422
Bore Radius	mm	34
B at Pole tip	T	0.354
Conductor	mm	5x5 , Dia. 3
Turns per Coil		28
Current	A	143
Current Density	A/mm ²	13.13
Resistance/coil	Ω	0.02752
Power Con./coil	kW	0.56
Temp. Change	°C	20
Pressure Drop	bar	1.05
Water Flow	L/min	1.5

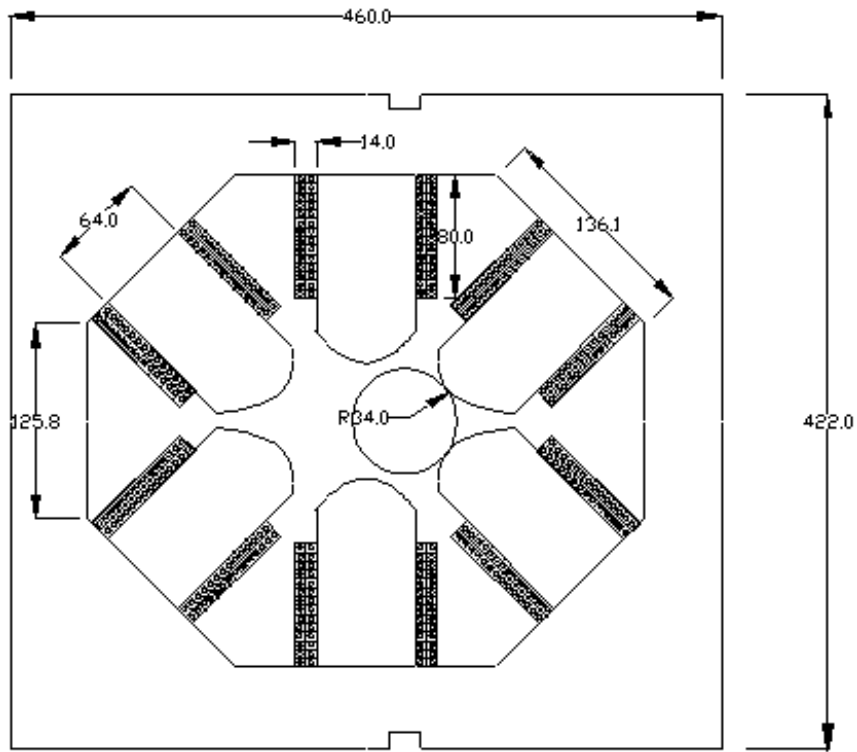


Figure 6.8: The Combined Sextupole-Quadrupole Magnet

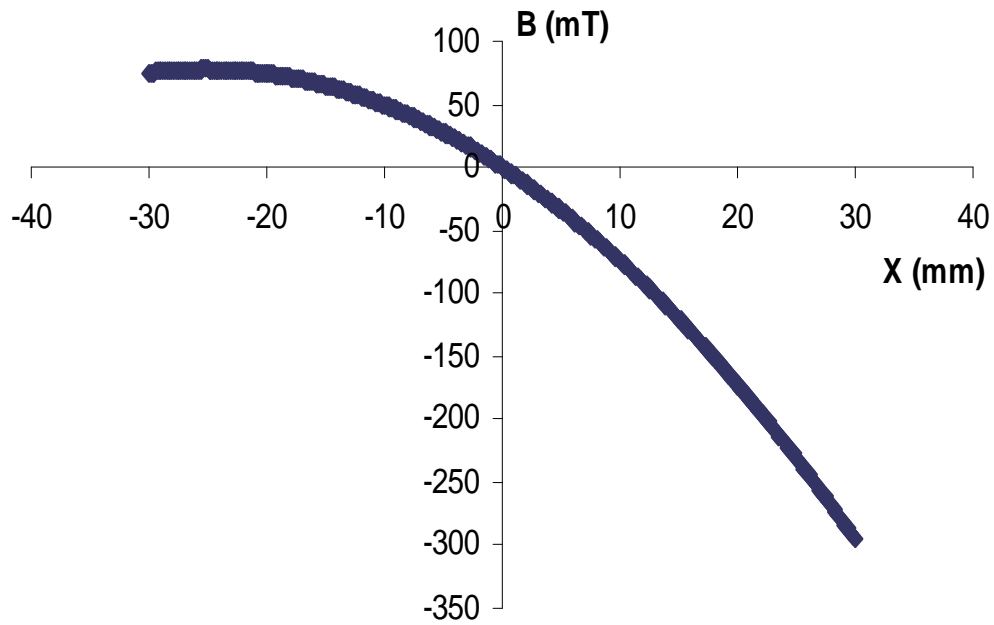


Figure 6.9: Magnetic field distribution at 2 (GeV) with $-6.17 (T/m)$ and $-122.4 (T/m^2)$

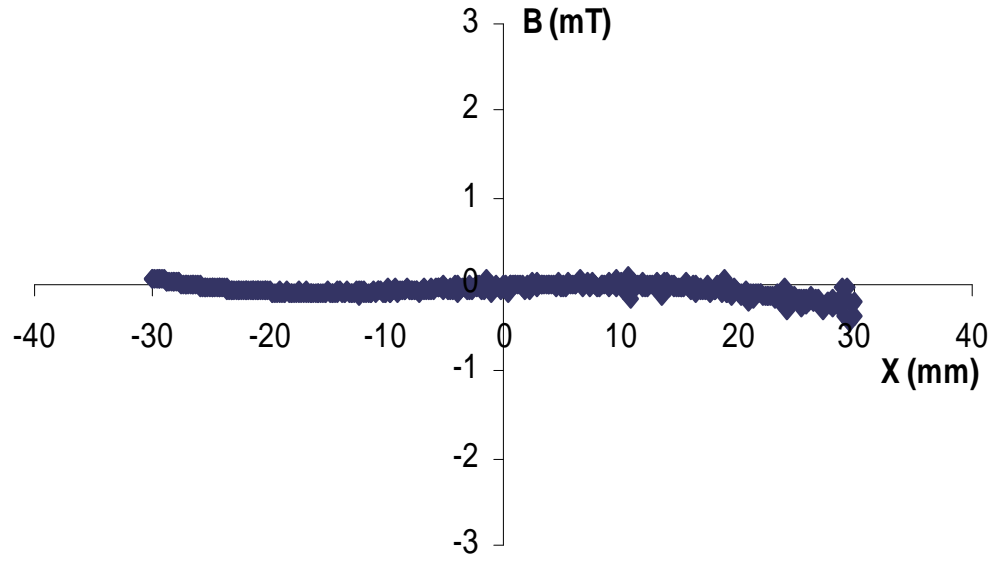


Figure 6.10: The residual field of the higher harmonics at 2 GeV

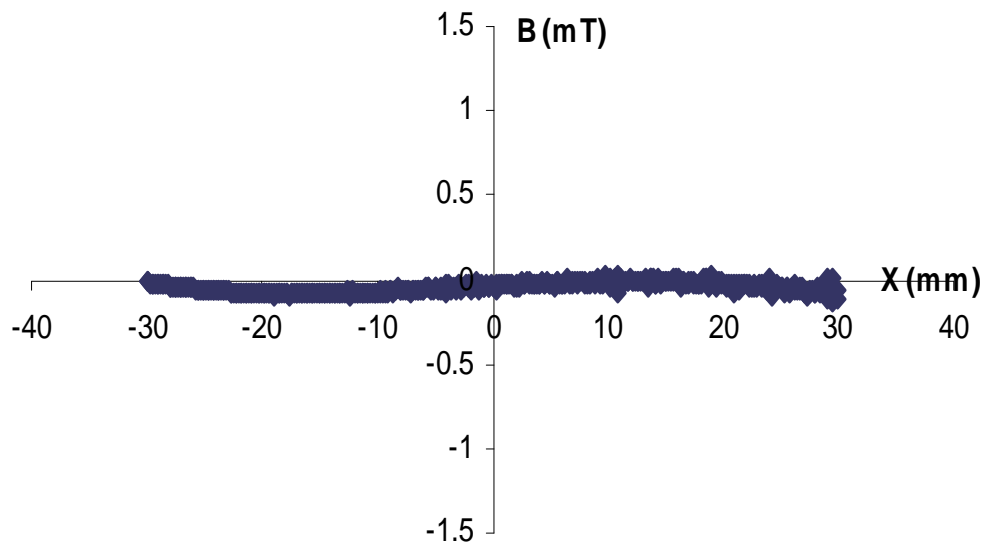


Figure 6.11: The residual field of the higher harmonics at 0.8 GeV injection energy

Table 6.5a: The calculated pole profile for the upper pole of the bending magnet

X (mm)	Y (mm)	X (mm)	Y (mm)	X (mm)	Y (mm)
0	20.07	44	21.682	-24	19.29
2	20.14	46	21.76	-26	19.23
4	20.2	48	21.84	-28	19.17
6	20.28	50	21.47	-30	19.11
8	20.35	52	21.15	-32	19.05
10	20.42	54	21.234	-34	18.99
12	20.49	56	21.316	-36	18.93
14	20.56	58	21.4	-38	18.86
16	20.63	59.8	21.8	-40	18.8
18	20.7	60.9	22.6	-42	18.75
20	20.774	60.9	22.6	-44	18.68
22	20.85	-2	20	-46	18.63
24	20.92	-4	19.94	-48	18.57
26	20.994	-6	19.87	-50	17.66
28	21.07	-8	19.8	-52	17.61
30	21.14	-10	19.74	-54	17.55
32	21.22	-12	19.676	-56	17.49
34	21.29	-14	19.61	-58	17.43
36	21.37	-16	19.55	-59	17.5
38	21.45	-18	19.48	-59.8	17.7
40	21.53	-20	19.42	-60.6	18.6
42	21.6	-22	19.36	-60.6	18.6

Table 6.5b: The calculated pole profiles for the upper three poles of the combined magnet

X (mm)	Y (mm)	X (mm)	Y (mm)	X (mm)	Y (mm)
71.59	5.1	2.84	52.8775	-57.16	57.52
68.84	4.96	-0.16	49.656	-72.8279	46.6379
64.84	5.45	-1.16	48.6615	-72.16	40.0114
62.84	5.7	-3.16	46.801	-72.16	38.8422
59.84	6.17	-5.16	45.1042	-72.66	32.9509
57.84	6.5	-7.16	43.5783	-73.16	30.5101
54.84	7.066	-10.16	41.61	-73.66	28.7221
51.84	7.699	-13.16	40.02	-74.16	27.2723
49.84	8.173	-16.16	38.799	-76.16	23.2213
46.84	8.98	-19.16	37.9422	-78.16	20.3711
43.84	9.91	-21.16	37.5555	-80.16	18.1891
40.84	11.0188	-24.16	37.2557	-83.16	15.7157
37.84	12.3461	-25.16	37.2298	-86.16	13.771
34.84	13.9693	-26.16	37.2407	-89.16	12.2138
32.84	15.2724	-27.16	37.3584	-91.16	11.3352
29.84	17.7	-30.16	37.8741	-93.16	10.5578
27.84	19.782	-34.16	38.8904	-96.16	9.54645
24.84	24.163	-38.16	40.5345	-100.16	8.42532
22.84	29.0187	-41.16	42.1978	-103.16	7.71779
21.84	33.5349	-45.16	45.0086	-106.16	7.10125
21.44	38.3673	-48.16	47.5654	-110.16	6.39415
21.84	45.966	-50.16	49.4799	-112.16	6.08183
6.84	57.685	-53.16	52.6535	-121.16	4.93673
4.84	55.2127	-56.16	56.1654	-121.91	5.1

6.6 Girders System

For the girder system it is foreseen to use the same one as for the storage rings ANKA and the SLS. The girders for ANKA are given in the following figures:

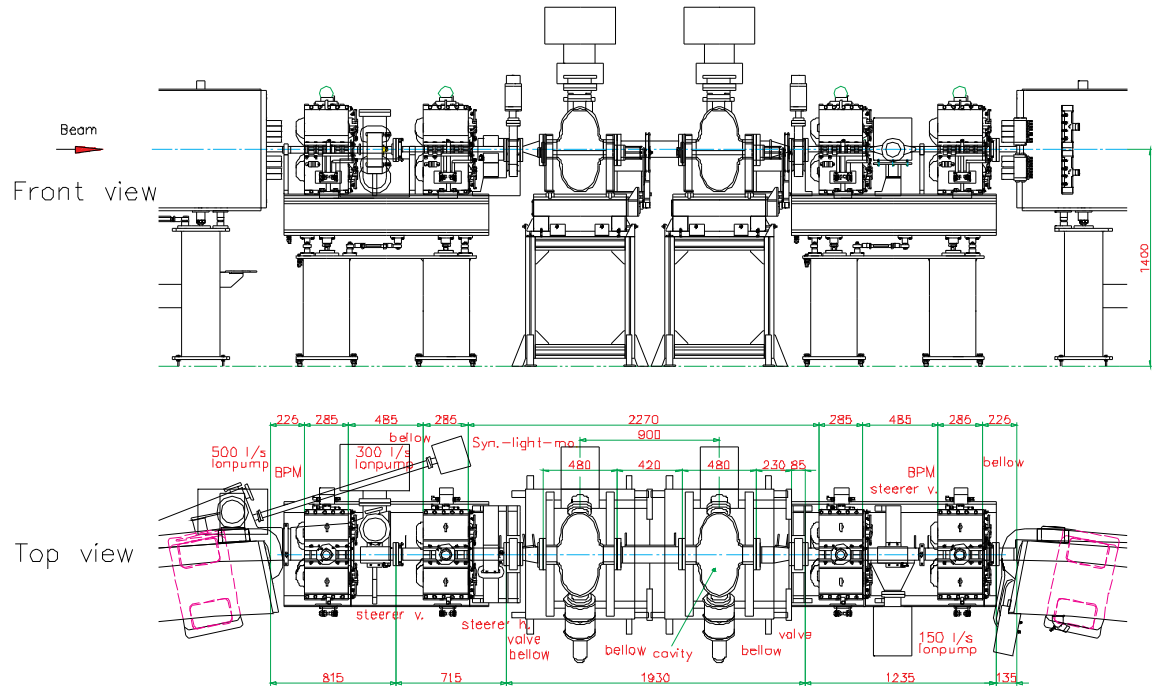


Figure 6.12: Girders of the RF-section for the storage ring ANKA

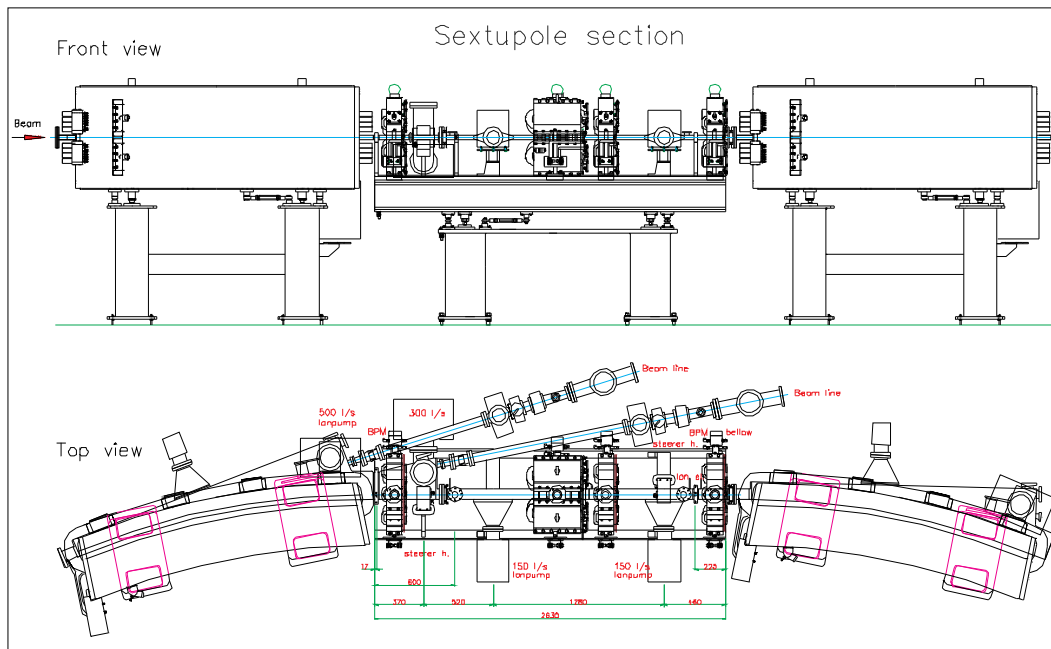


Figure 6.13: Girder of the dispersion sector for the storage ring ANKA

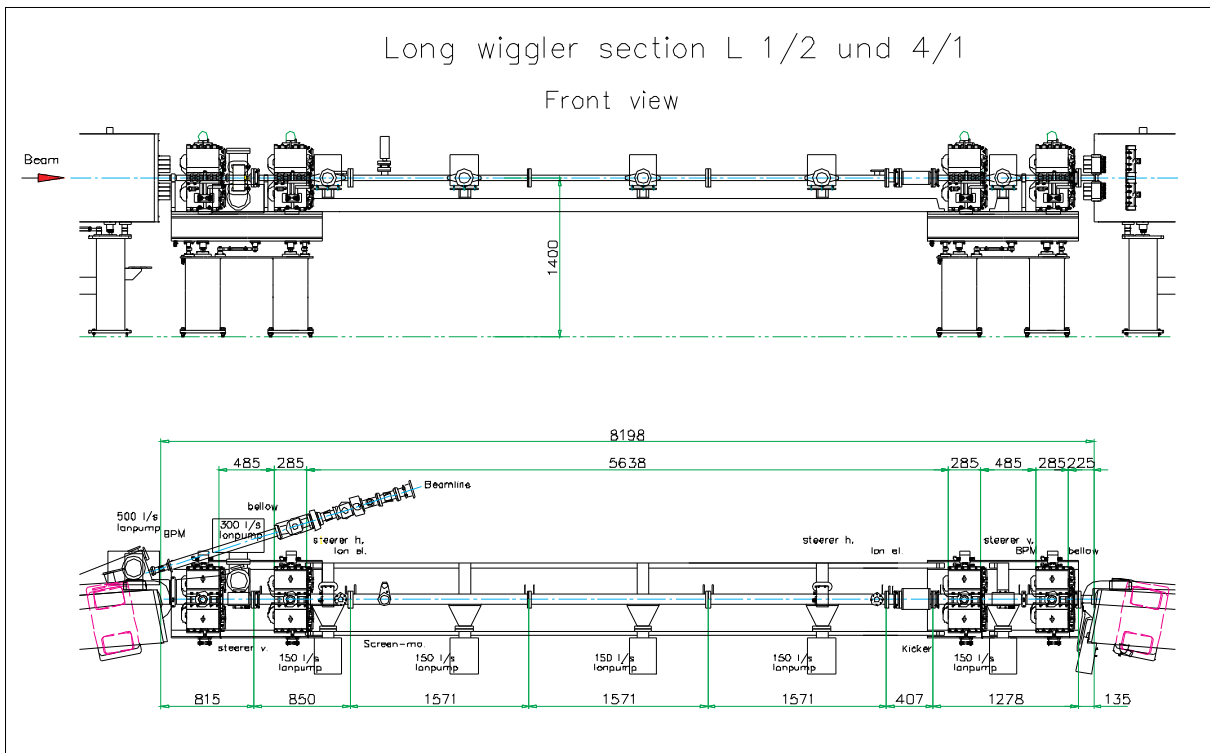


Figure 6.14: Girder of the long straight section for the storage ring ANKA

References

- [1] Å. Andersson et al, “*Design report for the MAX II ring*”, NTMX-7019,(1992)
- [2] David Meeker, “*Finite Element Method Magnetics*”, (FEMM code) version 3.0